J. Phys. Res. Edu., Vol. 2, March 2025

Calorimetric study of an induced nematic to smectic A phase transition in a binary system of two smectogens: Existence of double tricritical points

Apsari Parvin and Malay Kumar Das*

Department of Physics, University of North Bengal,

Raja Ramohunpur, 734013, Darjeeling, India

In this work, we investigate a series of binary mixtures comprising two smectogenic compounds, 5DBT (containing terminal group, NCS and exhibiting smectic A1 phase) and 10OCB (having terminal group, CN and exhibiting smectic Ad phase). The binary system exhibits an induced N (nematic) phase within a definite concentration limit between X_{5DBT} = 0.05 and X_{5DBT} = 0.95. Utilizing high-resolution MDSC setup, we have carried out a detailed heat capacity measurement at the induced N to smectic A (SmA) transition. Analysis of the latent heat confirms the occurrence of two tricritical points: one having the McMillan ratio = 0.981 and the other corresponding to 0.983. A distinct pretransitional heat capacity change close to the transition temperature is observed. The renormalization group theory involving a correction-to-scaling factor, effectively describes this anomaly. The critical exponent α follows a distinct pattern when plotted against both mole fraction (X_{5DBT}) and McMillan ratio (T_{NA}/T_{IN}). As the system approaches the tricritical point (TCP), a consistent shift from 2^{nd} order to 1^{st} order N–SmA transition is noticed on each end of the phase diagram. Both the TCP shares a common McMillan ratio = 0.982. Additionally, the 3D–XY model is precisely attained near X_{5DBT} = 0.687, corresponding to T_{NA}/T_{IN} = 0.909.

I. INTRODUCTION

The experimental and theoretical exploration on the character of phase transitional and physical characteristics of liquid crystal materials facilitates an enhanced insight into the mesomorphic nature of the liquid crystals (LCs). Those studies attain special consideration not only in the technological aspects [1, 2] but also for their basic understanding of the phase transition and critical phenomenon [3–6]. There is no single LC compound that fulfills the specification of even the simplest liquid crystal application. To obtain the desirable LC properties such as dielectric anisotropy, rotational viscosity, elastic constants, birefringence, etc. meeting the specifications for several applications, mesogenic compounds are mixed together. Moreover, in liquid crystal research, various phase transitions as well as critical phenomena are also studied using those mixtures [3–6].

One of the most interesting phenomena reported experimentally for the bi-component LC mixtures com-

prising two smectogenic compounds is the introduction of a new lower-ordered liquid crystalline phase commonly known as induced nematic phases [7–10]. Alternatively, many bi-component mixtures comprising two nematogens have been studied in which an induced smectic phase was noticed [11–13]. Binary mixtures frequently exhibit induced mesophase when one compound has a sturdily polar terminal group and another one is nonpolar [13–16], or both are polar nematic compounds [17–19]. The induction of new mesophases can be caused by the specific interaction between the two different molecules and is related to the construction of molecular complexes.

Numerous phase transitions in LCs have been analyzed to test the universal conceptions of critical phenomena and phase transitions. In this perspective, the nematic (N) to smectic A (SmA) transition plays a crucial role owing to the diverse phenomenology influenced by the continuous or discontinuous character of such transition, a property shaped by the N range of the investigated material [20, 21]. Specifically, the N width of smectogens characterizes the coupling intensity amid the N and SmA order parameters, which establishes the crossover from a continuous to a discontinuous nature of transition through a TCP [20]. The transition between the N and SmA phases has been examined widely, although it continues to be one of the most motivating challenges in condensed matter physics owing to a lack of consistency between the various reported data. Theoretically, the N-SmA transition was predicted to fit in the 3D XY universality class [22]. But, various studies have exposed a nonuniversal critical nature. Utilizing the mean-field hypothesis, Kobayashi [23], McMillan [24], and de Gennes [22] assumed a shift from 2^{nd} order to 1^{st} order transition at the TCP. The conjectural restraining value of McMillan ratio (T_{NA}/T_{IN}) at the TCP is anticipated to be 0.87, here, T_{NA} and T_{IN} are the N-SmA and N-isotropic transition temperatures correspondingly. So when T_{NA}/T_{IN} is higher than the restrictive assessment, the N–SmA transition becomes 1^{st} order, whereas, lower than this threshold it becomes 2^{nd} order. Till now observations confirm that the TCP does not display confirmation of a single universal assessment for the T_{NA}/T_{IN}, it lies in between 0.942 and 0.994. Utilizing the Landau free energy expression, de Gennes [22] demonstrated, a small nematic region leads to strong coupling amid the N and SmA order parameter, making N-SmA transition 1^{st} order, while, a larger N width weakens the coupling and driving the transition to become 2^{nd} order. Alternatively, Halperin, Lubenski, and Ma proposed that the N-SmA phase transition inevitably be weakly 1^{st} order if it incorporates the coupling between the nematic director fluctuation and the smectic A order parameter [25, 26]. Several mechanisms are used to modify the coupling power; one of the most widely used processes is to modulate the nematic width by preparing the bi-component mixtures.

In this paper a binary system of 5DBT and 10OCB has been analyzed to better comprehend the critical character of the N-SmA transition based on high-resolution heat capacity study, utilizing MDSC (modulated differential scanning calorimetry). Here an induced N phase has been observed, making it quite interesting

as both the pure materials display the smectic phase only. Phase diagram, dipole moments, static dielectric parameters, and density measurement for a series of these concentrations have previously been reported [27]. Investigations of optical birefringence and refractive indices have already been performed to identify the behaviour of the N-SmA transition [28]. The observed order parameters are adequately analogous to those calculated using McMillan's theory [24, 29]. The critical exponent α related to the N–SmA transition gives information related to critical behaviour of the transition, thereby enabling us to situate the TCP precisely.

II. EXPERIMENTAL

A. Materials

A systematic investigation on a series of binary mixtures comprising compounds, 5DBT, having an NCS terminal group and 10OCB, with a CN terminal group is presented. 5DBT was procured from Poland (AWAT Co. Ltd.), whereas 10OCB was obtained from UK (E. Merck) and utilized as received. Both the liquid crystal compounds display a single mesophase, the smectic A phase. The chemical names, along with molecular structural formulae, phase sequences and phase transition temperatures, of the pure compounds under investigation are provided below (Fig. 1).

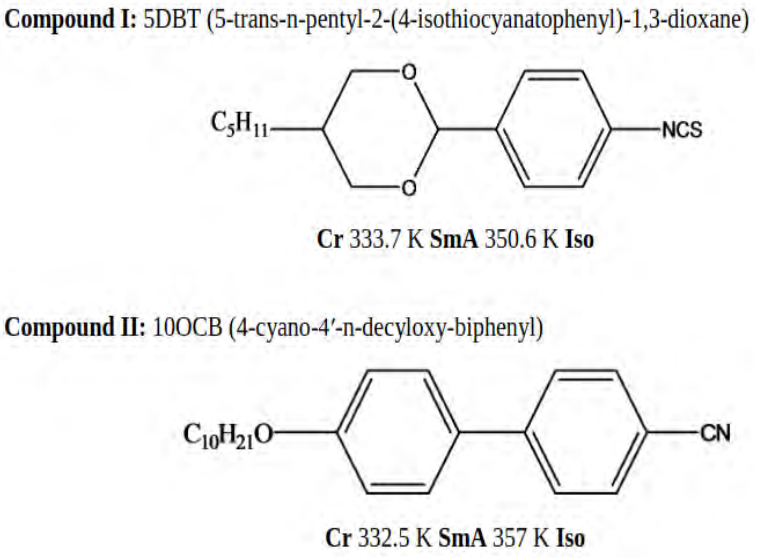

FIG. 1. Two different liquid crystal compounds.

The bi-component mixtures are denoted as X_{5DBT}, representing the molar fraction of 5DBT in 10OCB. Total nine binary mixtures were prepared with X_{5DBT} values equal to 0.10, 0.16, 0.20, 0.25, 0.69, 0.74,

0.80, 0.89, and 0.95. The temperatures linked to phase transition of the pure samples and their binary mixtures were determined through high-resolution MDSC study. A heating or cooling rate = 0.5 K/min was employed to the samples.

B. Specific heat capacity measurement

The MDSC technique was utilized to conduct measurements, operating as a conventional DSC or in modulated mode. MDSC is an enhanced variant of normal DSC, which provides precise temperature variation of specific heat capacity. A linear temperature ramp is superposed during modulation mode, with sinusoidal temperature variation, to introduce a perturbation. The MDSC technique works under three investigational factors: temperature amplitude modulation, heating or cooling rate, and the period of oscillation. A thorough discussion of this technique utilized in this study is documented elsewhere [30–32]. For this work, a high-resolution differential scanning calorimeter (Model: DSCQ2000, TA instruments, USA), with a refrigerating cooling equipment, was used, operating within the temperature range of 183 K to 823 K. Indium and pure synthetic sapphire were utilized to calibrate the specific heat with high precision. Throughout the experiment, a constant pressure was maintained by purging N_2 gas (dry) with 50 ml/min flow rate throughout the DSC cells. A small amount of the sample (5–10 mg) was taken to make sure a consistent thin layer inside the sealed Tzero aluminum pan. The MDSC method is appropriate for calculating latent heat in 1^{st} order phase transitions, including weakly 1^{st} order phase transitions. Along with heat capacity, MDSC also delivers phase shift (ϕ), aiding in determining the two-phase coexistence region in 1^{st} order as well as weakly 1^{st} order transitions.

III. RESULTS AND DISCUSSIONS

A. Phase diagram

The phase diagram of the 5DBT + 10OCB bi-component system derived from the MDSC study is displayed in Fig 2(a). Both the pure compounds 5DBT and 10OCB exhibit the following stable phase sequence: Cr–SmA–Iso. Although they are purely smectogenic in nature, an induced N phase appears in the concentration limit $0.10 \leq X_{5DBT} \leq 0.95$. However, in the concentration limit $0.25 \leq X_{5DBT} \leq 0.69$, the SmA phase vanishes entirely and only the N phase exists. The phase transition temperatures, T_{IN} and T_{NA} identified from the calorimetric study, closely match with the formerly reported temperatures [27]. A close examination of Fig.2 demonstrates that the SmA phase completely disappears at the equimolar region, whereas, the SmA phase is highly stable in the areas where any of the pure compound is present in high

concentration. The most stable N phase is noticed for X_{5DBT} = 0.69. Also the nematic width variation with the molar concentration of 5DBT is depicted in Fig. 2(b).

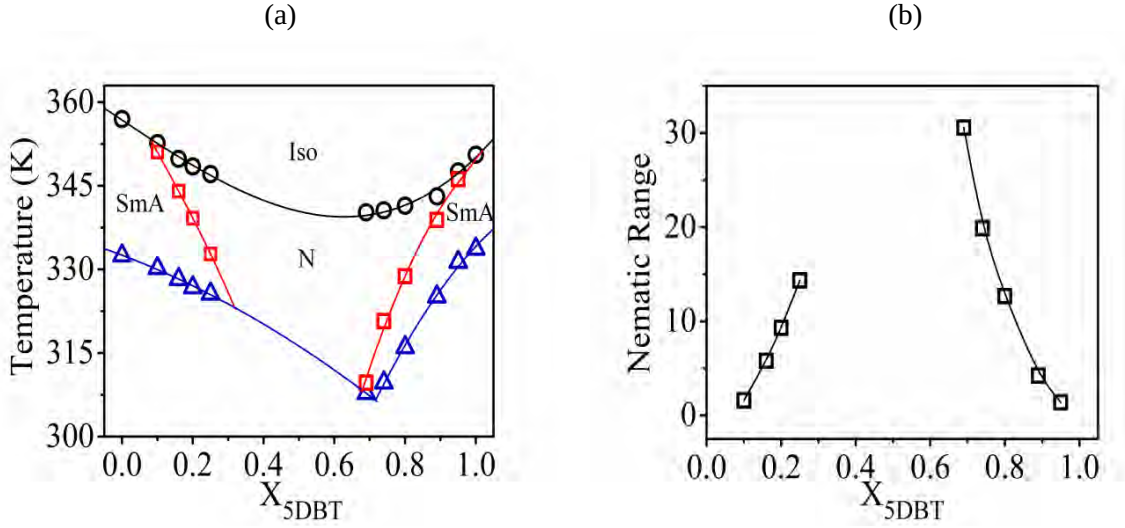

FIG. 2. (a) Phase diagram of 5DBT + 10OCB system, where, the molar concentration of 5DBT was denoted by X_{5DBT}. The phases are denoted as Iso (isotropic), SmA (smectic A), and N (nematic). (b) Variation of the N width with X_{5DBT}. Solid lines serve merely as visual guides.

B. Calorimetric measurements

The heat capacity measurements have been conducted for the 5DBT + 10OCB system across the whole temperature range spanning from isotropic to crystalline state during the cooling process from the isotropic state subjected to three conditions: (a) modulation amplitude ± 0.1 K, (b) scan rate 0.5 K/min, and (c) modulation time 10 s. For the studied mixtures, within the concentration limit of $0.10 \leq X_{5DBT} \leq 0.25$, and $0.69 \leq X_{5DBT} \leq 0.95$, two well-defined and discernible peaks of heat capacity indicative of the phase transitions are identified: Iso–N and N–SmA and the consequent transition temperatures (T_{IN}: Iso to induced N and T_{NA}: N to SmA) were precisely recognized by monitoring the upper most value of the CP (T) peak during both heating and cooling cycles.

The latent heat (ΔH_L) near the N-SmA transition (measured using standard DSC experiments with 3 K/min scan rate throughout both heating and cooling cycles) are presented against McMillan ratio (T_{NA}/T_{IN}) in Fig. 3(a) and 3(b) and the corresponding molar concentration (X_{5DBT}) dependent ΔH_L data are presented in insets of Fig. 3(a) and 3(b). The release of energy (ΔH_L) throughout the N-SmA transition initially decreases with the increase in X_{5DBT}, approaching a minimum in close proximity to

$X_{5DBT} \approx 0.171$ and increases after $X_{5DBT} \approx 0.859$. ΔH_L has been employed to accurately extort the probable tricritical concentrations correlated to N-SmA phase transition; this can be employed to detect a crossover in the behaviour of transition from 1^{st} order to 2^{nd} order. Current bi-component system exhibits two TCP concentrations for the N-SmA transition are recognized through extrapolation. The 1^{st} tricritical point has been experimentally detected at T_{NA}/T_{IN} = 0.981 and the 2^{nd} tricritical point exists at T_{NA}/T_{IN} = 0.983. However, the N-SmA transition peak is clearly detected for compositions beyond both the tricritical points. Hence, the initial assessment of the order of phase transition has been determined based on the observed enthalpy change. The MDSC technique is suitable for determining both specific heat capacity

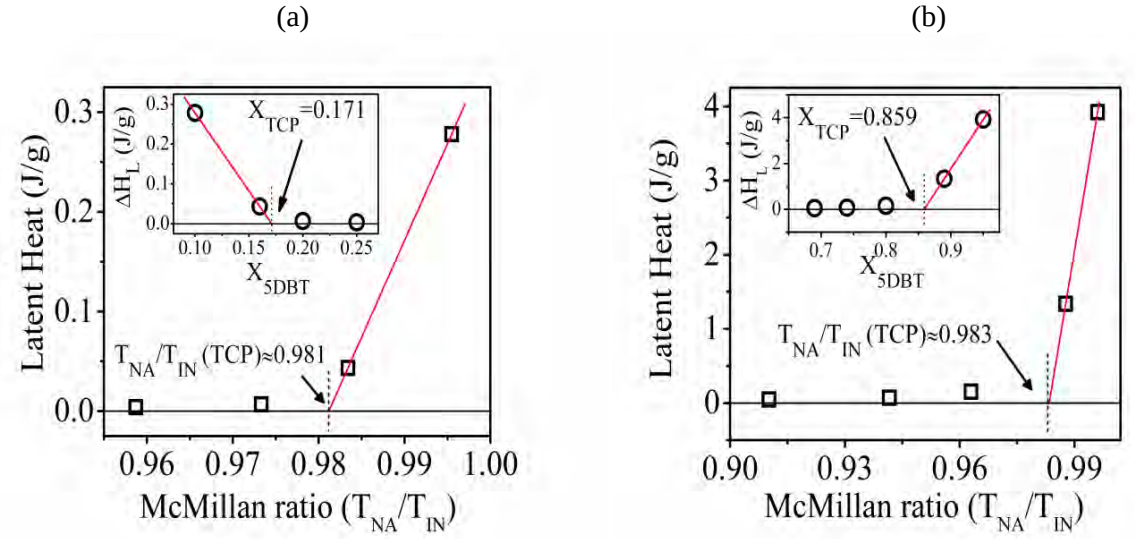

FIG. 3. McMillan ratio (T_{NA}/T_{IN}) dependence of latent heat (ΔH_L) near the N-SmA phase transition for mixtures with (a) X_{5DBT} = 0.10, 0.16, 0.20, and 0.25; (b) 0.69, 0.74, 0.80, 0.89, and 0.95. The corresponding molar concentration (X_{5DBT}) dependent latent heat data are presented in respective insets. Red solid lines signify linear fit to the values, whereas, black dotted lines indicate the tricritical points.

($\Delta C_p = C_p - C_{p,\text{background}}$) and consequent phase shift (ϕ) data. The 1^{st} order phase transition shows a distinct peak in ϕ, analogous to the ΔC_p peak, whereas, a 2^{nd} order transition shows either a gradual dip or no significant phase shift change [4, 5, 33]. The non-reversible heat capacity component ($\Delta C_p''$) is linked to the heat capacity release, and also indicates the order of phase transition. In 1^{st} order transition, ($\Delta C_p''$) may oscillate owing to the occurrence of ϕ in the coexistence region, as determined through Fourier analysis [34]. While at 2^{nd} order transition ($\Delta C_p''$) shows either no peak or a minimal change, indicating negligible ΔH_L. Figure 4(a) and 4(b) depict the observed ΔC_p, corresponding imaginary component of ΔC_p ($\Delta C_p''$), and phase shift (ϕ) at the N-SmA transition at various mole fractions of X_{5DBT} for all the studied mixture. The quick rise in specific heat, near the N-SmA transition of the 5DBT + 10OCB system close to the phase

diagram's edges implies the strong 1^{st} order transition, whose effectiveness gradually diminishes near the central region of the phase diagram. The phase transitional order as well as the subsistence of tricritical concentration for the N-SmA transition can be determined utilizing the $\Delta C_p''$ and corresponding variation in phase shift (ϕ) with temperature for various mixtures.

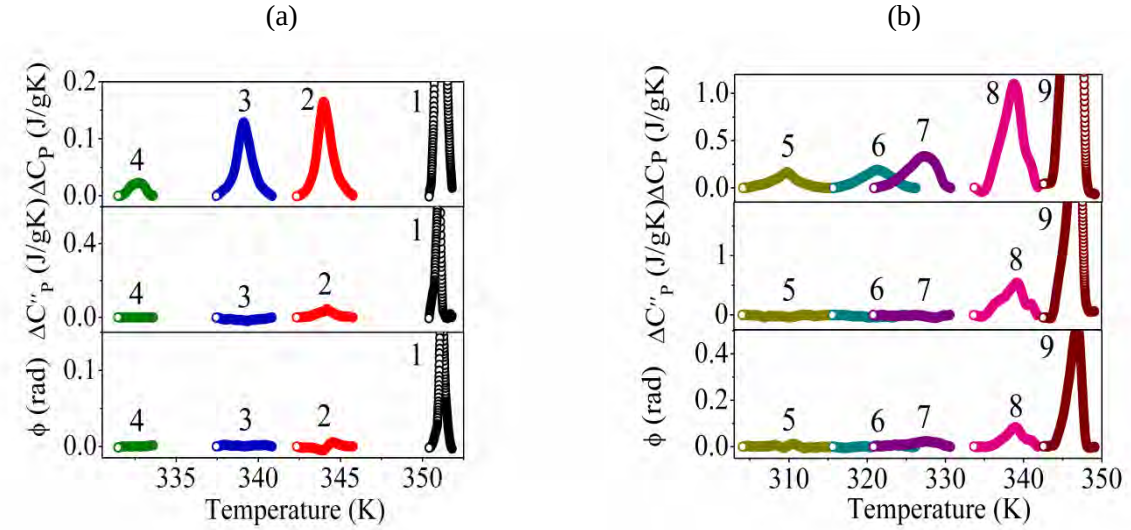

FIG. 4. Heat capacity (ΔC_p), imaginary part of ΔC_p $(\Delta C_p'')$, and phase shift (ϕ) as a function of temperature in close proximity to the N-SmA transition for various X5DBT. Data displayed with 1: X_{5DBT}=0.10; 2: X_{5DBT}= 0.16; 3: X_{5DBT}=0.20; 4: X_{5DBT}=0.25; 5: X_{5DBT}=0.69; 6: X_{5DBT}=0.74; 7: X_{5DBT}=0.80; 8: X_{5DBT}= 0.89; 9: X_{5DBT}=0.95.

For the studied mixtures X_{5DBT} = 0.10, 0.16, 0.89, and 0.95 the pattern of the peak related to $\Delta C_p''$ and phase shift (ϕ) is almost identical to the peak in heat capacity, signifying a phase transition of 1^{st} order. Although, for X_{5DBT} = 0.20, 0.25, 0.69, 0.74, and 0.80 the phase shift (ϕ) and $\Delta C_p''$ are almost vanished.

C. Critical behaviour near the N-SmA transition using renormalization group theory

Generally, binary systems composed of both nonpolar and polar materials demonstrated Fisher renormalization [4, 35]. In this work, both the compounds are polar, consequently, no sign of Fisher renormalization is anticipated. Furthermore, one can validate this by analyzing the gradient of the lnT_{NA} versus the concentration (x) curve. Fisher renormalization is anticipated to happen when the slope $[d(ln\ T_{NA})/dx]^2$ falls within the range of 0.74 to 9.0, and for a small slope, Fisher renormalization does not occur [4, 35]. In this system, the value of $[d(ln\ T_{NA})/dx]^2$ is observed to lie within the range of 0.02 to 0.49. Such a minute value of the slope implies that this bi-component system is entirely free from the Fisher renormalization.

The N-SmA phase transition in the analyzed mesomorphic system exhibits a pronounced critical variance in the high-resolution heat capacity measurement. The temperature dependence of ΔC_p near the N-SmA transition has been investigated using the succeeding renormalization group expression [4, 36–38],

$$\Delta C_p(T) = \frac{A^{\pm}}{\alpha}|\tau|^{-\alpha}(1 + D^{\pm}|\tau|^{\Delta}) + E|\tau| + B^{\pm}, \quad (1)$$

where $\tau = (T - T_{NA})/T_{NA}$, $\pm$ denotes terms corresponding to above and below T_{NA}, $A^{\pm}$ represents the critical amplitudes, $D^{\pm}$ are the coefficients of the 1^{st} corrections–to–scaling conditions, Δ is the exponent for the 1^{st} corrections–to–scaling expressions, α is the critical exponent of the ΔC_p, $B^{\pm}$ denotes the combined invariable for critical and standard background contributions. Additionally, $E|\tau|$ accounts for the temperature-dependent portion within the standard background contribution. Initially, we treated Δ as a free parameter and the superiority of the fits was decided through X_v^2, the reduced error function [39, 40]. Our investigation acknowledged that the error function achieves its minimum or nearly minimum value when Δ is set to 0.5. Consequently, we fixed Δ at 0.5 without additional variation for subsequent analysis. The fitted parameter values are displayed in Table I and the consequent fitted curves are represented by red solid lines in Fig. 5.

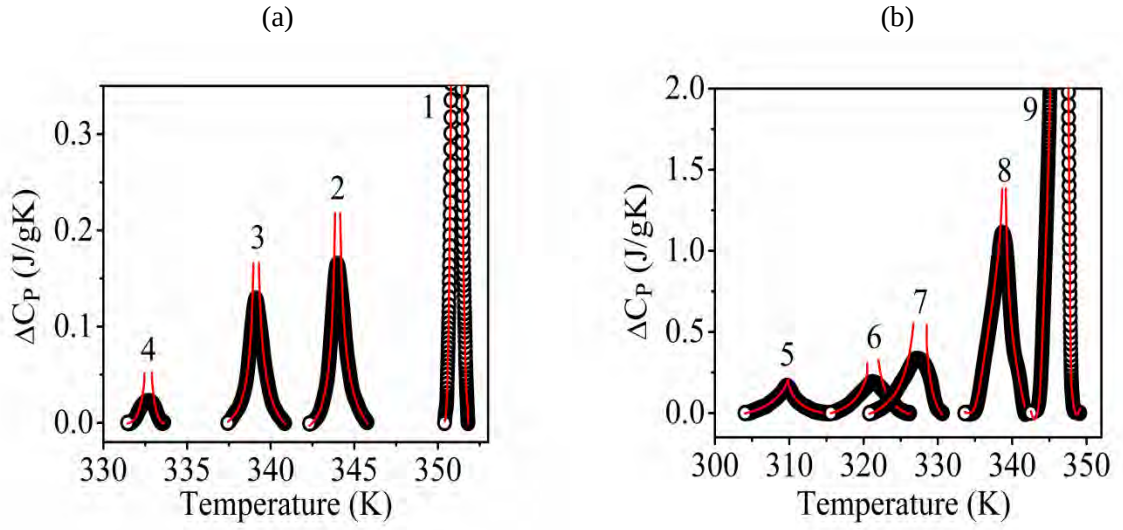

FIG. 5. Temperature-dependent heat capacity (ΔC_p) in the proximity of the N–SmA transition at various mole fractions of X5DBT. Data displayed with 1: X5DBT = 0.10; 2: X5DBT = 0.16; 3: X5DBT =0.20; 4: X5DBT = 0.25; 5: X5DBT = 0.69; 6: X5DBT = 0.74; 7: X5DBT = 0.80; 8: X5DBT = 0.89; 9: X5DBT = 0.95. Solid red lines stand for fit to Equation 1.

In practice, data are selected and analyzed only within a restricted limit of reduced temperature. Initially, values around TNA are discarded to evade the effects of rounding region, where the data typically deviate

X_{5DBT}	$\|\tau\|_{\max} \times 10^3$	A^-/A^+	D^-/D^+	α	X_v^2
0.10	2.0	1.021 ± 0.052	1.024 ± 0.051	0.506 ± 0.001	1.14
0.16	5.0	1.006 ± 0.046	1.001 ± 0.042	0.503 ± 0.001	1.13
0.20	5.0	1.001 ± 0.019	1.069 ± 0.038	0.418 ± 0.015	1.17
0.25	3.5	1.001 ± 0.029	1.010 ± 0.018	0.319 ± 0.028	1.45
0.69	18.0	1.011 ± 0.036	1.022 ± 0.020	-0.007 ± 0.011	1.06
0.74	16.5	1.014 ± 0.026	1.009 ± 0.013	0.196 ± 0.006	1.27
0.80	15.0	0.994 ± 0.015	1.002 ± 0.086	0.344 ± 0.017	1.21
0.89	12.0	1.008 ± 0.029	0.999 ± 0.029	0.501 ± 0.001	1.19
0.95	9.5	1.001 ± 0.020	1.003 ± 0.019	0.502 ± 0.001	1.08

h!

TABLE I. Characteristic parameters consequent to the best fit for CP in the neighborhood of the N-SmA transition according to Equation (1) and allied X_v^2 values connected to the fits; $|\tau|_{\max}$ describe the maximum boundary of the reduced temperature range used for the fits.

from the theoretical model. Consequently, the parameters are selected to maximize the number of data points while minimizing the remaining standard deviation, ensuring the uniformity between the theoretical models and experimental data. The temperature dependencies of $\Delta C_p(T)$ for all bi-component mixtures near the TNA are well described by Eq. (1), signifying a strong conformity between experimental data and the theoretical power law behavior examined here. The X_v^2 values range in between 1.06 to 1.45, signifying a strong fit to the considered model expression.

Figure 6 demonstrates the composition-dependent variation of the critical exponent α, the values are determined by averaging of those measured below and above the N-SmA transition. The α values offer crucial findings related to the order nature of the transition, enabling a precise identification of the tricritical concentration. Within the limit, $0.20 \leq X_{5DBT} \leq 0.80$, the α values remain below the tricritical threshold of 0.5, undoubtedly reflecting a phase transition of 2^{nd} order in these concentrations near the N–SmA phase. Conversely, for concentrations X_{5DBT} = 0.10 and 0.16, the α value nears the tricritical threshold, suggesting a 1^{st} order character of the N-SmA transition. Consequently, the probable shift between the 2^{nd} order to 1^{st} order behaviour of the N-SmA transition is likely to occur within the range of X_{5DBT} = 0.16 to 0.20. Meanwhile, for X_{5DBT} = 0.80, the exponent α is 0.344, whereas, for X_{5DBT} = 0.89, the exponent α becomes 0.501, suggesting the presence of another TCP within the concentration range of $0.80 \leq X_{5DBT} \leq 0.89$ in this studied system. Figure 6 indicates, the extrapolated concentrations at which the N-SmA phase transition making a changeover from 2^{nd} order to 1^{st} order i.e., the TCPs are established to be at X_{5DBT} = 0.171 and 0.857, on opposite edges of the phase diagram.

The critical exponent data for all concentrations exhibit a clear and consistent prototype when plotted

with respect to T_{NA}/T_{IN}, as demonstrated in Fig. 6. A 2^{nd} order polynomial fit to the data provides a TCP value of 0.982 for the McMillan ratio (T_{NA}/T_{IN}), at which α = 0.5. For $T_{NA}/T_{IN} > 0.982$, the coupling between the N and SmA order characters is sufficiently strong to induce a weak 1^{st} order N-SmA transition. Furthermore, with $\alpha = -0.0068 \pm 0.011$, the 3D-XY model is nearly approached (the hypothetical value is $\alpha = -0.007$) at $X_{5DBT} = 0.687$, corresponding to $T_{NA}/T_{IN} = 0.909$. A thorough inspection of Fig. 6 reveals three key findings: (a) a strong correlation is evident between the critical exponent α and T_{NA}/T_{IN}, (b) at $T_{NA}/T_{IN} = 0.982$, the tricritical point occurs on each edges of the phase diagram for the analyzed system. When T_{NA}/T_{IN} exceeds 0.982, the N-SmA transition is 1^{st} order and lower this threshold, it becomes 2^{nd} order and (c) the investigated system encompasses all 1^{st} ordered, tricritical, and 3D-XY compositions.

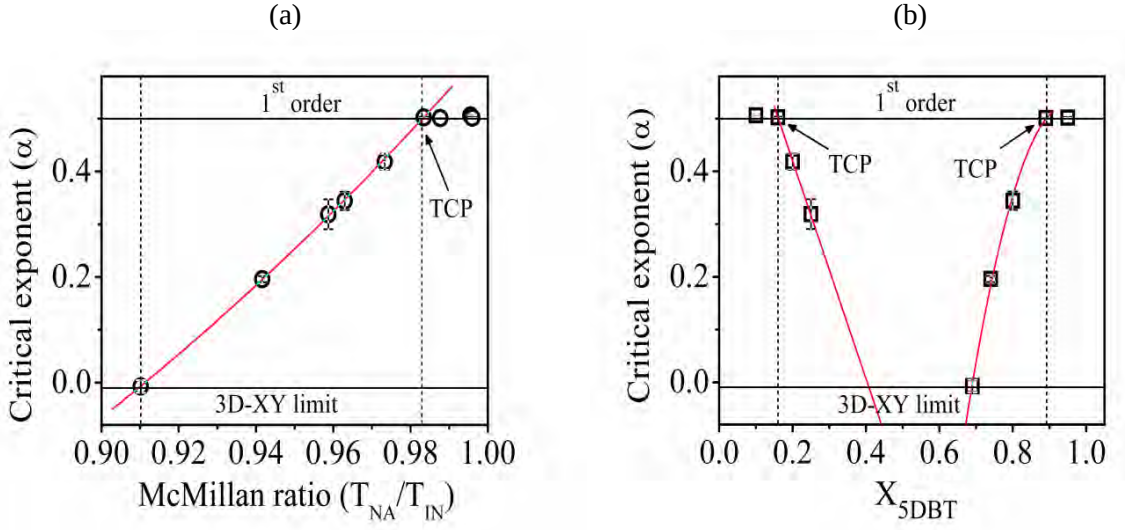

FIG. 6. Dependence of critical exponent (α) on (a) McMillan ratio (T_{NA}/T_{IN}) and (b) molar concentration (X_{5DBT}) obtained from MDSC measurement near the N-SmA transition. Red lines represent polynomial fit to the α values.

IV. CONCLUSIONS

In this work, high-resolution calorimetric investigations are performed on a bi-component system of smectogens that exhibits an induced N phase. This scheme proves to be a promising model for exploring the phase transition and corresponding critical behaviour in the realm of soft condensed matter physics. As the composition of either pure compounds deviates toward higher or lower values, the nematic region contracts and stability of the SmA phase is enhanced. Toward the phase diagram centre, the SmA phase vanishes entirely, with N phase remaining only. Special attention was given to the excess $\Delta C_p(T)$ and latent heat

data near the N-SmA phase transition to determine the phase transitional order in the studied bi-component system. The N-SmA phase transition is predominantly 2^{nd} order, with the exception of X_{5DBT} = 0.10, 0.16, 0.89, and 0.95, where the N-SmA transition becomes 1^{st} order. It is observed that a decrease in nematic width of the mixtures corresponds to an increase in the critical exponent (α). Moreover, a few critical exponents are positioned between the 3D–XY class and the TCP. A noble characteristic of this system is the subsistence of two TCPs, each on either side of the phase diagram, occurring at $X_{5DBT} \approx 0.171$ and 0.859 for the N-SmA transition, making a changeover from 2^{nd} order to 1^{st} order transition. Amusingly, the McMillan ratios for the two TCP concentrations converge precisely at $T_{NA}/T_{IN} = 0.982$. Additionally, for $\alpha = 0.0068 \pm 0.011$, the 3D-XY model is achieved almost accurately at $X_{5DBT} = 0.687$, corresponding to a McMillan ratio of $T_{NA}/T_{IN} = 0.909$.

ACKNOWLEDGEMENTS

AP extends heartfelt appreciation to the University Grants Commission for granting an SRF award [UGC/NFOBC/201920-19J6148547].

* mkdnbu@nbu.ac.in

[1] M. Roushdy, Liq. Cryst. **31**, 371 (2004).
[2] B. Bahadur, Mol. Cryst. Liq. Cryst. **109**, 3 (1984).
[3] M. A. Anisimov, Critical phenomena in liquids and liquid crystals, UK, ch. **10**, 305 (1991).
[4] M. B. Sied, J. Salud, D. O. Lopez, M. Barrio, and J. L1. Tamarit, Phys. Chem. Chem. Phys. **4**, 2587 (2002).
[5] M. B. Sied, S. Diez, J. Salud, D. O. Lopez, P. Cusmin, J. L1. Tamarit, and M. Barrio, J. Phys. Chem. B **109**, 16284 (2005).
[6] M. G. Lafouresse, M. B. Sied, H. Allouchi, D. O. Lopez, J. Salud, and J. L1. Tamarit, Chem. Phys. Lett. **376**, 188 (2003).
[7] R. Dabrowski, and J. Szulc, J. Phys. France **45**, 1213 (1984).
[8] R. Dabrowski, and K. Czuprynski, Mol. Cryst. Liq. Cryst. **146**, 341 (1987).
[9] K. Czuprynski, R. Dabrowski and J. Przedmojski, Mol. Cryst. Liq. Cryst., Lett. Sect. **4**, 429 (1989).
[10] K. Czuprynski, R. Dabrowski, J. Baran, A. Zywocinski and J. Przedmojski, J. Phys. France **47**, 1577 (1986).
[11] H. Sackmann and D. Demus, Z. Phys. Chem. (Leipzig) **230**, 285 (1965).
[12] W. H. de Jeu, L. Longa and D. Demus, J. Chem. Phys. **84**, 6410 (1986).
[13] C. S. Oh, Mol. Cryst. Liq. Cryst. **42**, 1 (1977).
[14] P. E. Cladis, Mol. Cryst. Liq. Cryst. **67**, 177 (1981).
[15] P. D. Roy, A. Prasad and M. K. Das, J. Phys.: Condens. Matter **21**, 075106 (2009).

[16] A. Parvin and M. K. Das, Phase Trans. **96**, 746, (2023).

[17] M. Brodzik and R. Dabrowski, Liq. Cryst. **18**, 61 (1995).

[18] S. Wrobel, M. Brodzik, R. Dabrowski, B. Gestblom, H. Hasse and S. Hiller, Mol. Cryst. Liq. Cryst. **302**, 223 (1997).

[19] M. Tykarska, B. Wazynska and I. Ulbin, Proc. of the SPIE, Poland **4147**, 55 (2000).

[20] C. W. Garland and G. Nounesis, Phys. Rev. E **49**, 2964 (1994).

[21] E. Anesta, G. S. Iannacchione, and C. W. Garland, Phys. Rev. E **70**, 041703 (2004).

[22] P. G. de Gennes and J. Prost, The Physics of liquid crystals, Clarendon, Oxford, 2nd ed, (1993).

[23] K. K. Kobayashi, Theory of translational and orientational melting with application of liquid crystals. I, Phys. Lett. A 31, 125 (1970).

[24] W. L. McMillan, Phys. Rev. A **4**, 1238 (1971).

[25] B. I. Halperin, T. C. Lubensky and S. K. Ma, Phys. Rev. Lett. **32**, 292 (1974).

[26] B. I. Halperin and T. C. Lubensky, Solid State Commun. **14**, 997 (1974).

[27] S. K. Sarkar, and M. K. Das, Fluid Phase Equilibria **365**, 41 (2014).

[28] S. K. Sarkar, and M. K. Das, RSC Advances **4**, 19861 (2014).

[29] W. L. McMillan, Phys. Rev. A **6**, 936 (1972).

[30] B. Wunderlich, A. Boller, I. Okazaki, and K. Ishikiriyama, Thermochim Acta **304–305**, 125 (1997).

[31] P. Cusmin, M. R. de la Fuente, J. Salud, M. A. Pérez-Jubindo, S. Diez-Berart, and D. O. Lopez, J. Phys. Chem. B **111**, 8974 (2007).

[32] J. Salud, D. O. Lopez, S. Diez-Berart, and M. R. de la Fuente, Liq. Cryst. **40**, 293 (2013).

[33] S. Diez, D. O. Lopez, M. R. de la Fuente, M. A. Pérez-Jubindo, J. Salud, and J. Ll. Tamarit, J. Phys. Chem. B **109**, 23209 (2005).

[34] P. Kalakonda, H. Kashuri, K. Kashuri and G. S. Innacchione, Indian J. Pure and Appl. Phys. **52**, 689, (2014).

[35] K. J. Stine, and C. W. Garland, Phys. Rev. A **39**, 1482 (1989).

[36] M. B. Sied, D. O. Lopez, J. L1. Tamarit, and M. Barrio, Liq. Cryst. **29**, 57 (2002).

[37] C. W. Garland, Liquid crystals: Experimental study of physical properties and phase transitions, (Cambridge University Press) (2001).

[38] J. A. Potton, and P. Lanchester, Phase Transit. **6**, 43 (1985).

[39] P. R. Bevington and D. K. Robinson, Data reduction and error analysis for the Physical Sciences, 3rd ed. (McGraw-Hill) (2003).

[40] A. Zywocinski, J. Phys. Chem. B **107**, 9491, (2003).

